

01NVSOQ – Advanced Antenna Engineering

ASSIGNMENT 4: ARRAY COMPONENTS

Amedeo Bertone (243878)
Davide Botteon (239595)
Enrico Maria Renzi (244028)

January 11, 2018

Contents

1	Introduction	1
2	Problem no.1	2
2.1	Splitter 1 design	4
2.2	Splitters2,3 and match2 design	7
2.3	Match2 design	11
2.4	Complete BFN with dimensions	13
3	Problem no.2	19
3.1	Simulation with <i>Design Studio</i>	19
3.2	Simulation with <i>Microwave Studio</i>	22
4	Problem no.3	24

1 Introduction

The goal of this project is the realization of the Beam Forming Network able to provide the right feeding to an array of four elements which should exhibit a tapering able to shape the array factor so that the SLL is lower than -20 dB (exercise 2 of the previous assignment)..

This first part (definition of inter-element spacing and tapering) was already carried out during the previous assignment and leaded us to choose the values that we will use during the rest of the project.

In particular, the first part of the work deals with the handmade project of the BFN in order to obtain the correct power ratios for the four radiators, which are the patches we designed in the second assignment (resonance at 2.45 GHz and $120\ \Omega$ input impedance), the correct phasing, 0 in order to

obtain a broadside array, and an input impedance of $50\ \Omega$. All these specs should be met at 2.45 GHz and in the largest possible band around this frequency. In this part, simulation of the single parts of the BFN are also provided, in order to get a glimpse on the correct or not correct behavior of the final version.

The second part is related to the simulation of the BFN. It is worth to anticipate from the very beginning that this part turned out to be very tricky, since in a first moment, through the use of *CST Design Studio* we seemed to confirm our design and even optimize it in a good way, but later on we encountered lots of difficulties in replicating such results in *CST Microwave Studio*, which poses lots of difficulties in the optimization due to the very long simulation time, dense meshes and huge weight of all the non linearities and non idealities. In fact, even if the single parts of our BFN work in a reasonable way when standalone, they do not work so well when they are put together.

The third and last part deals with the simulation of the radiating structure of the array. First, a further optimization of the single patch was carried out, in order to get the most close as possible to the prescribed $120\ \Omega$ impedance and 2.45 GHz resonance. Then, the patches are put together in order to verify how they behave when assembled in order to form the array, to see how they mutually influence each other. We have to mention that even in this case simulation was not straightforward and the problems encountered in the second part about long simulation time and difficulty on tuning were present even in this case, so that the results hopefully should be, even in this case, susceptible to further perfecting.

2 Problem no.1

Here is presented the design of a corporate beam forming network. By specification, FR4 is given as substrate (the technological specifications follow in table 1).

The antenna's radiating part requires four radiators with cosine-over-pedestal tapering, hence the BFN is symmetric with respect to the feeding

Table 1: FR4 technological specifications.

Quantity	Symbol	value	
Dielectric permittivity	ϵ_r	4.3	
Substrate height	h	1.5	mm
Metal thickness	t	0.1	mm
Minimum strip width	W_{\min}	0.15	mm
Minimum spacing between lines	Δs_{\min}	0.175	mm

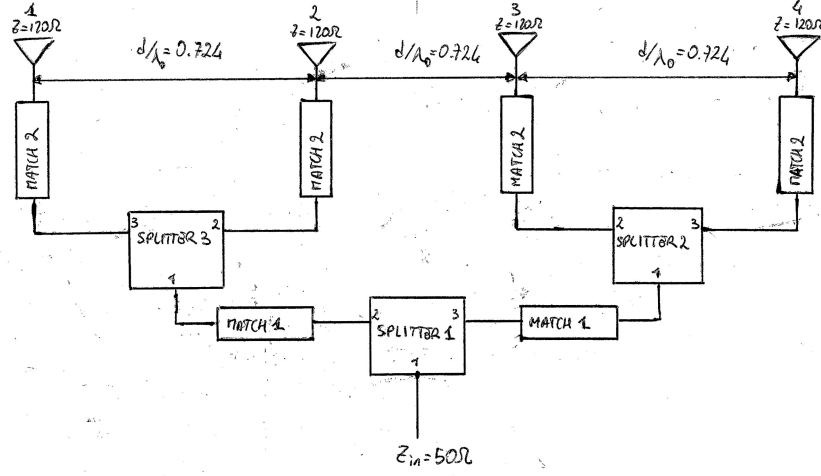


Figure 1: Beam forming network's block diagram.

line.

One possible implementation is proposed in figure 1, where the building blocks can be identified as follows:

Splitter1 this section matches the input line to $Z_{in}=50\Omega$ at the input port. Moreover, it evenly splits the power into two branches that follows, therefore this is a 3dB splitter.

Splitter2 this section matches the radiating elements with section1 outputs, moreover it convey power into the radiators giving the correct power ratio between elements.

Splitter3 this is symmetric to section2 with respect to the feeding line longitudinal axis.

Match1 these lines acts as matching connection from power splitter1 to power splitters2 and 3, moreover they are used to adjust the distance between elements.

Match2 matching connections between radiators and power splitters2,3;

Overall the BFN should be designed in order to be compliant with the requirement on:

- grating lobes, related to the element spacing d ($d/\lambda_0 = 0.724$);
- amplitude tapering between edge and centre elements;
- main beam direction: since the array is broadside then the phase shift among elements must be null.

Another requirement concerns the full array's dimensions, although those are not specified particular attention will be devoted into taking the minimal amount of space. Each block's design and simulation are reported in the following paragraphs.

2.1 Splitter 1 design

Figure 2 shows the block diagram of splitter1.

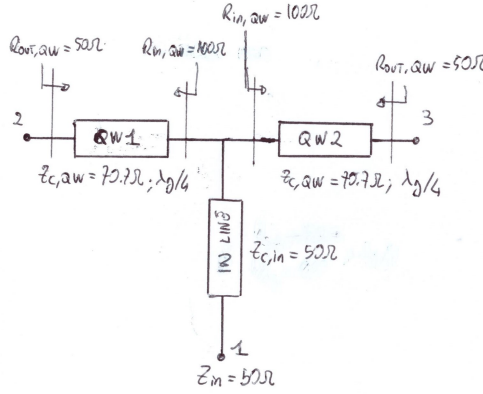


Figure 2: Splitter1 TXL implementation.

The input line is power matched to the input port by means of a 50Ω line whose length has been chosen arbitrarily. To evenly split the power into port 2 and 3 we use a T-junction made up of two quarter-wavelength transformers. This components show real input and output impedance and the following relation for their characteristic impedance holds:

$$Z_{c,QW} = R_{c,QW} = \frac{1}{G_{c,QW}} = \sqrt{R_{in,QW} \cdot R_{out,QW}} \quad (1)$$

As a first approximation, the two quarter-wavelength transformers are seen as two parallel admittances from the input port, then to have the 50Ω matching we have:

$$G_{c,QW1} + G_{c,QW2} = \frac{1}{Z_{in}} = \frac{1}{50\Omega} \Rightarrow Z_{c,QW1} = Z_{c,QW2} = Z_{c,QW} = 100\Omega$$

Willing to reduce impedance discontinuities within the network, the section's output impedance is set to 50Ω too, hence:

$$Z_{c,QW} = \sqrt{R_{in,QW} \cdot R_{out,QW}} = \sqrt{100\Omega \cdot 50\Omega} = 70.7\Omega$$

Finally the design has been converted from ideal microstrip lines to physical

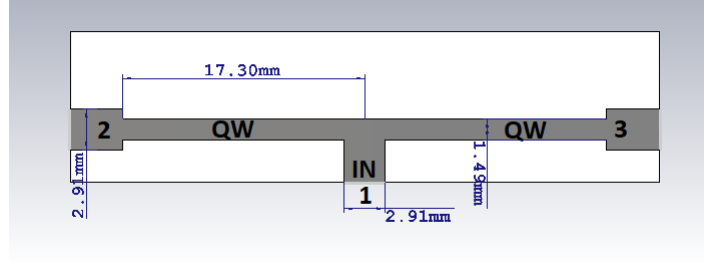


Figure 3: Splitter1 microstrip implementation.

lines by means of TX-LINE: Transmission Line Calculator (from NI AWR Design Environment) and eventually implemented in CST DS™ for the optimization process. Theoretical and optimized dimensions are reported in table 2 and 3. The resulting scattering parameters are shown in figure 4: both power splitting and phase behaves as expected. Figure 3 depicts the microstrip implementation of this section.

Table 2: Splitter1: Input line dimensions

	theoretical	optimized	
W_{in}	3.02	2.91	mm
$Z_{c,in}$	50	50.06	Ω

Table 3: Splitter1: quarter-wavelength transformer dimensions

	theoretical	optimized	
W_{QW}	1.59	1.49	mm
L_{QW}	17.25	17.3	mm
$Z_{c,QW}$	70.7	73.1	Ω

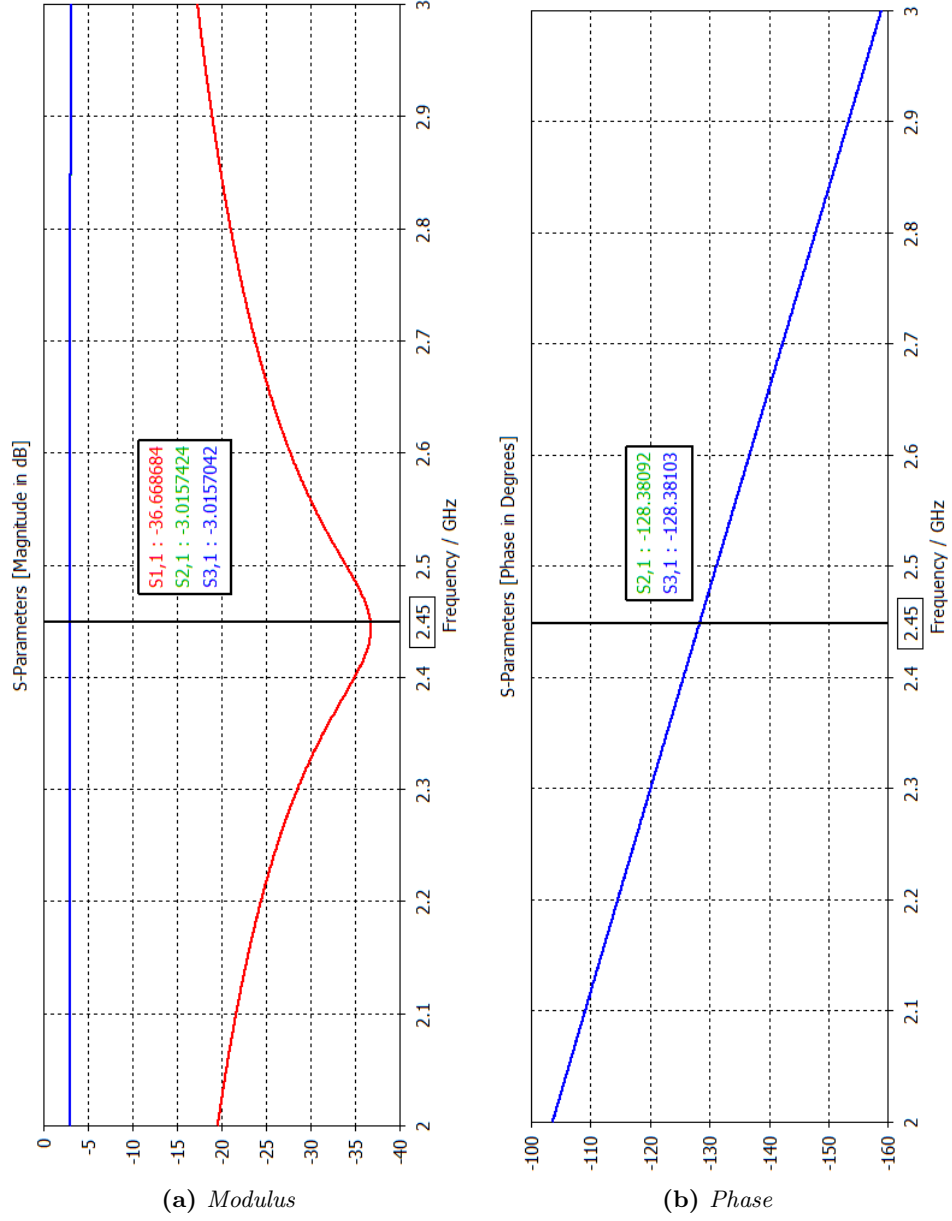


Figure 4: Section 1 most important scattering parameters. As it appears both input matching and even power splitting are accomplished, the phase shift is null (reference impedance 50Ω).

2.2 Splitters2,3 and match2 design

Figure 5 shows the block diagram of splitter2 and match1 (splitter3 is specular).

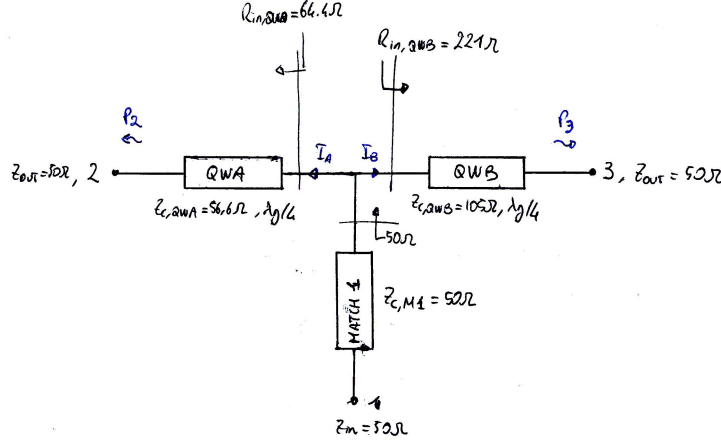


Figure 5: Splitter2 and match1 TXL implementation.

Match1 is designed as, 50Ω characteristic impedance line. Since both the output of splitter1 and the input of splitter2,3 are matched to 50Ω , the length of these line can be chosen as necessary to impose the correct distance between the radiators. Again, splitter2,3's output impedance is set to $Z_{out}=50\Omega$ to avoid abrupt mismatch in contiguous lines connections. Moreover, imposing $Z_{in}=50\Omega$ we also avoid the appearance of lines narrower than W_{min} within the two splitters.

Again, quarter-wavelength transformers are employed to provide the correct current tapering for the radiators, this time they act as uneven power divider. To design that we will consider the power entering and exiting the component. Having chosen as tapering $t=0.54$, then:

$$\frac{S_{31}}{S_{21}} = 0.54 \Rightarrow \frac{P_3}{P_2} = \left(\frac{S_{31}}{S_{21}} \right)^2 = 0.292 \Rightarrow \frac{P_3}{P_2} = -5.34dB$$

where S_{21} and S_{31} are the scattering transmission coefficients at port 2 and 3. In particular P_2 is the power exiting the splitter and directed to the centre element, whereas P_3 goes to the edge radiator (supposing lossless TXL):

$$\begin{cases} P_2 = P_a = \frac{1}{2} R_{in, QWA} |I_A|^2 \\ P_3 = P_b = \frac{1}{2} R_{in, QWB} |I_B|^2 \end{cases}$$

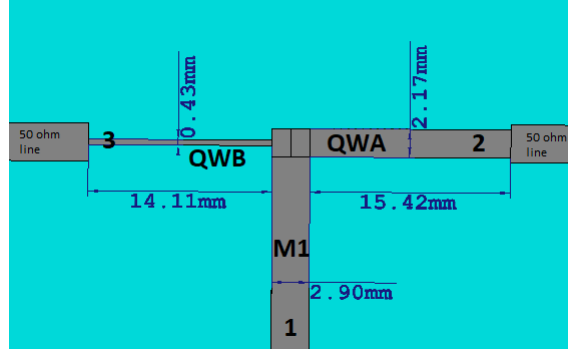


Figure 6: Splitter2 microstrip implementation.

As before, the two impedance transformers are seen as two in-parallel conductances from port 1, then the following system holds:

$$\begin{cases} \frac{1}{R_{in,QW_a}} + \frac{1}{R_{in,QW_b}} = \frac{1}{Z_{in}} \\ \frac{P_3}{P_2} = \frac{R_{in,QW_a}}{R_{in,QW_b}} = 0.292 \end{cases}$$

that has solutions:

$$R_{in,QW_b} = 221\Omega$$

$$R_{in,QW_a} = 64.6\Omega$$

From equation (1):

$$Z_{c,QW_b} = \sqrt{R_{in,QW_b} \cdot Z_{out}} = \sqrt{221\Omega \cdot 50\Omega} = 105\Omega$$

$$Z_{c,QW_a} = \sqrt{R_{in,QW_a} \cdot Z_{out}} = \sqrt{64.4\Omega \cdot 50\Omega} = 56.7\Omega$$

Finally, the circuit has been converted into microstrip layout and simulated. Some optimized dimensions for this section are reported in table 4 and 5 (Match1 has the same parameters shown in 2). The values found so far produced both the expected tapering and 3.46° of phase shift between branches. Figure 7 shows the input parameters, while figure 6 depicts the microstrip implementation.

Table 4: Splitter2: quarter-wavelength a dimensions.

	theoretical	optimized	
W_{QW_a}	2.44	2.17	mm
L_{QW_a}	16.96	15.42	mm
Z_{c,QW_a}	56.6	60.4	Ω

Table 5: Splitter2: quarter-wavelength b dimensions.

	theoretical	optimized	
W_{QW_b}	0.613	0.43	mm
L_{QW_b}	17.709	14.11	mm
Z_{c,QW_b}	105	118	Ω

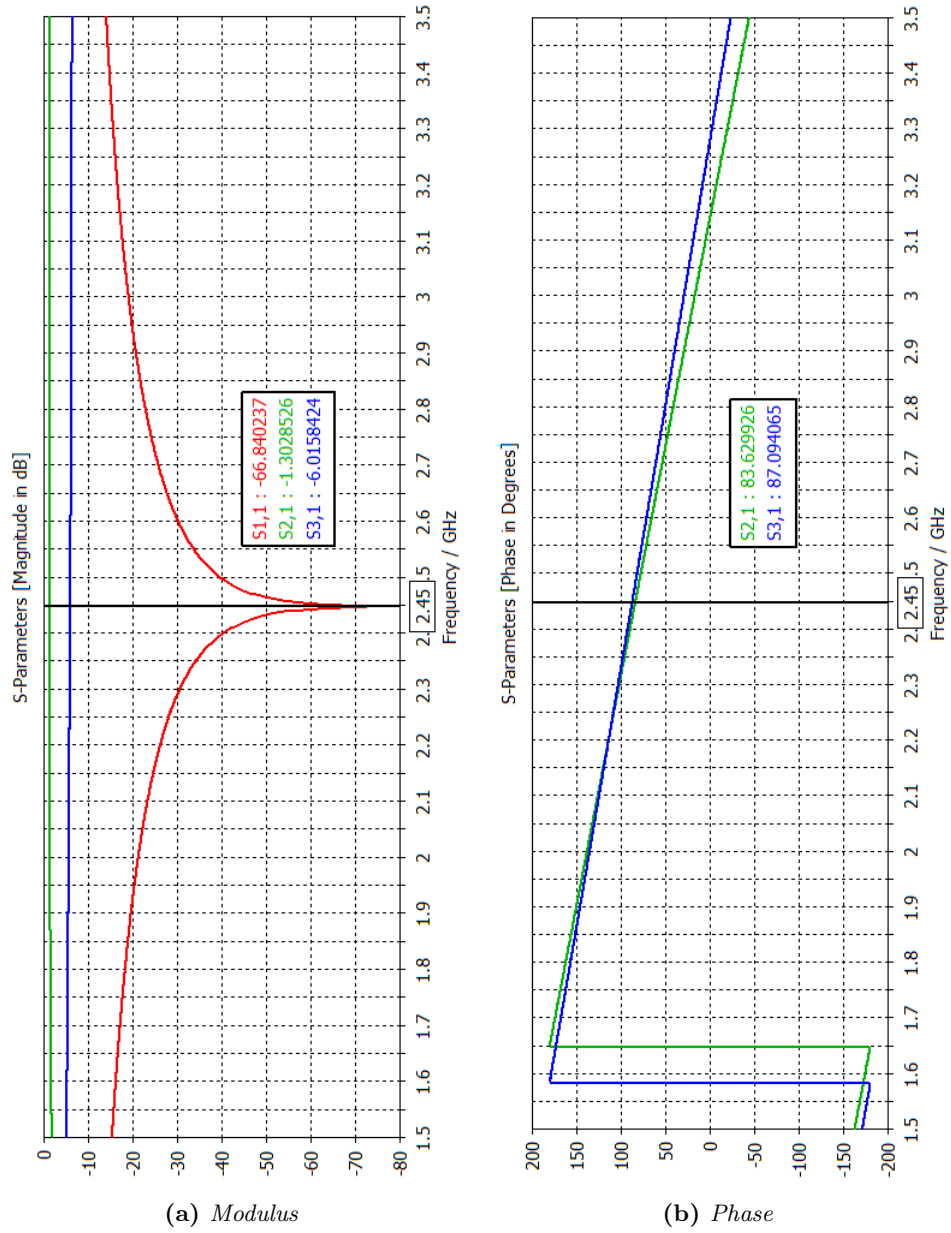


Figure 7: Section 1 most important scattering parameters. As it appears both input matching and even power splitting are accomplished. The tapering value is $t = -5.2$ dB, the phase shift amounts to 3.94° (reference impedance 50Ω).

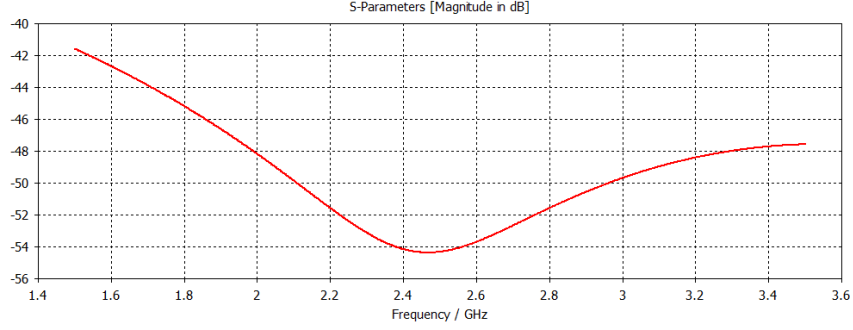


Figure 8: Match2 return loss (reference impedance 77.5Ω).

2.3 Match2 design

As final design step, another quarter-wavelength transformer is introduced. This element matches splitter2 and splitter3, $R_{out}=50\Omega$, output impedance with the radiators' input impedance, equal to $Z_{in,patch}=120\Omega$. Using equation (1) we have:

$$\begin{aligned}
 Z_{c,M2} &= \sqrt{R_{in,M2} \cdot R_{out,M2}} \\
 &= \sqrt{Z_{out} \cdot Z_{in,patch}} \\
 &= \sqrt{120\Omega \cdot 50\Omega} = 77.5\Omega
 \end{aligned}$$

The conversion from ideal microstrip to layout can be found in table 6, whereas the return loss is shown in figure 8

Table 6: Match2: microstrip dimensions.

	theoretical	optimized	
W_{M2}	1.32	1.21	mm
L_{M2}	17.37	17.37	mm
$Z_{c,M2}$	77.5	80.4	Ω

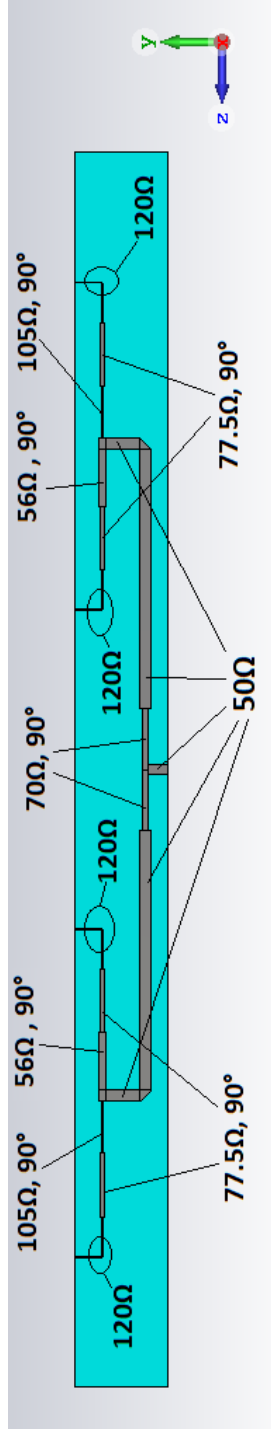


Figure 9: Full beam forming network.

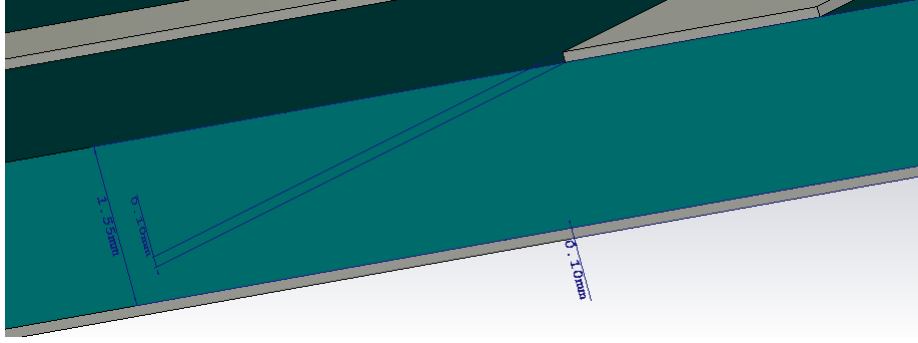


Figure 10: Here are highlighted the quoted regions.

2.4 Complete BFN with dimensions

Now that all the main components have been optimized the following step includes the merging of all the sections as shown if figure 9. To connect splitter1 with splitter2 we used a 50Ω line bent in order to be compliant with the radiators' spacing specification. The bend has been chosen with mitered topology, to reduce parasitics. Furthermore, the 50Ω and 120Ω lines parallel to the y axis are kept short to reduce the space occupied by the BFN. Finally the whole structure has been finely tuned and optimized to obtain the best performances. A full set of quoted schematics is grouped from figure 10 to figure 15. Within the following paragraph all the simulations will be presented.

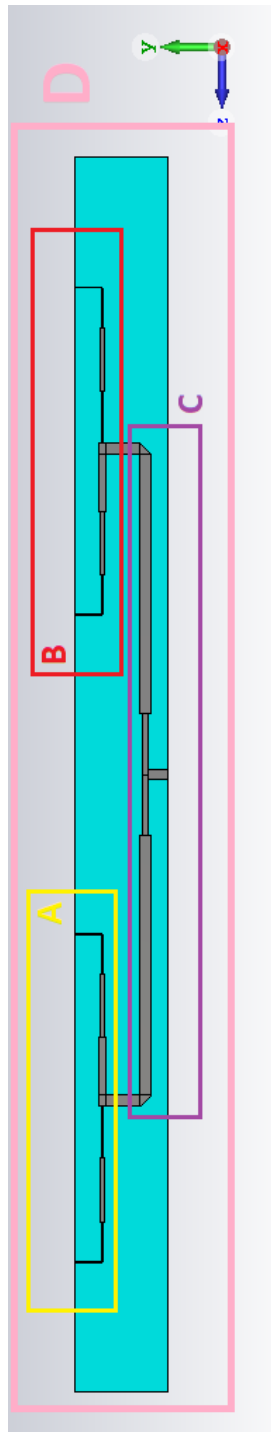


Figure 11: Here the quoted regions are highlighted.

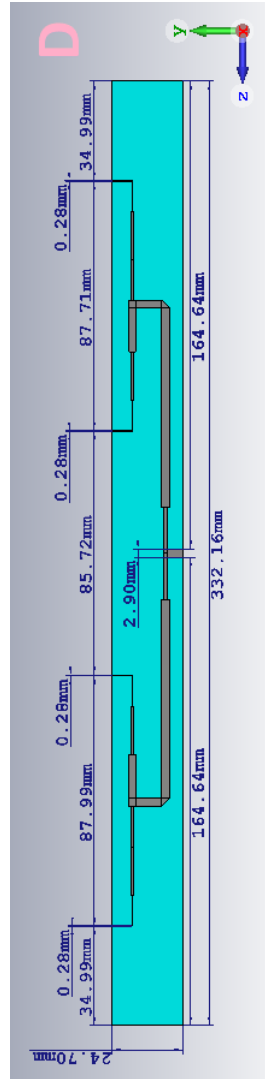


Figure 12: Quoted BFN: region D.

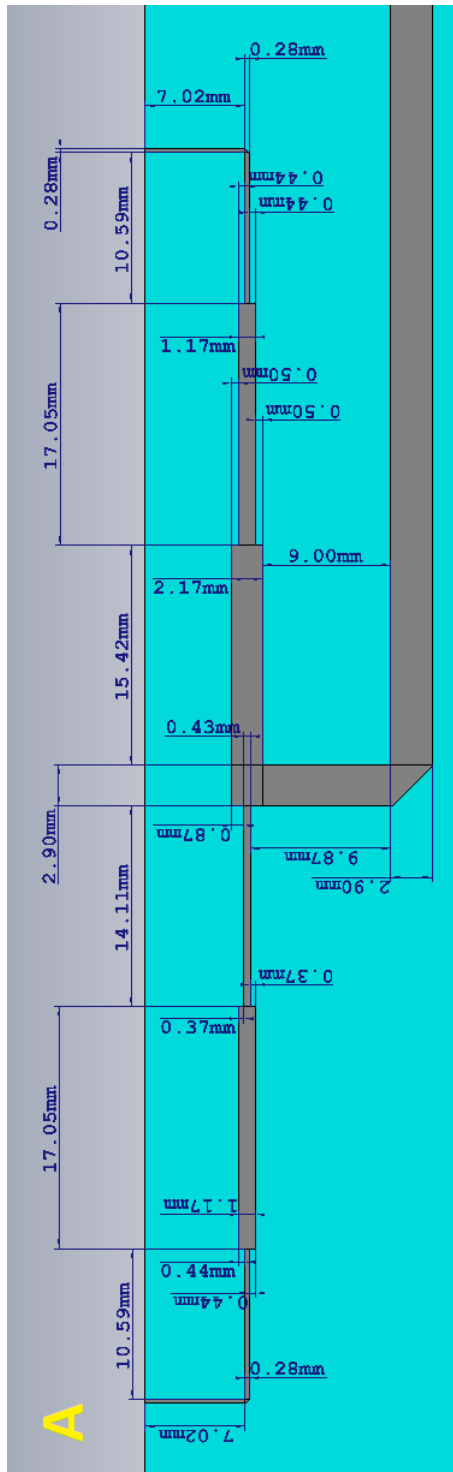


Figure 13: Quoted BFN: region A.

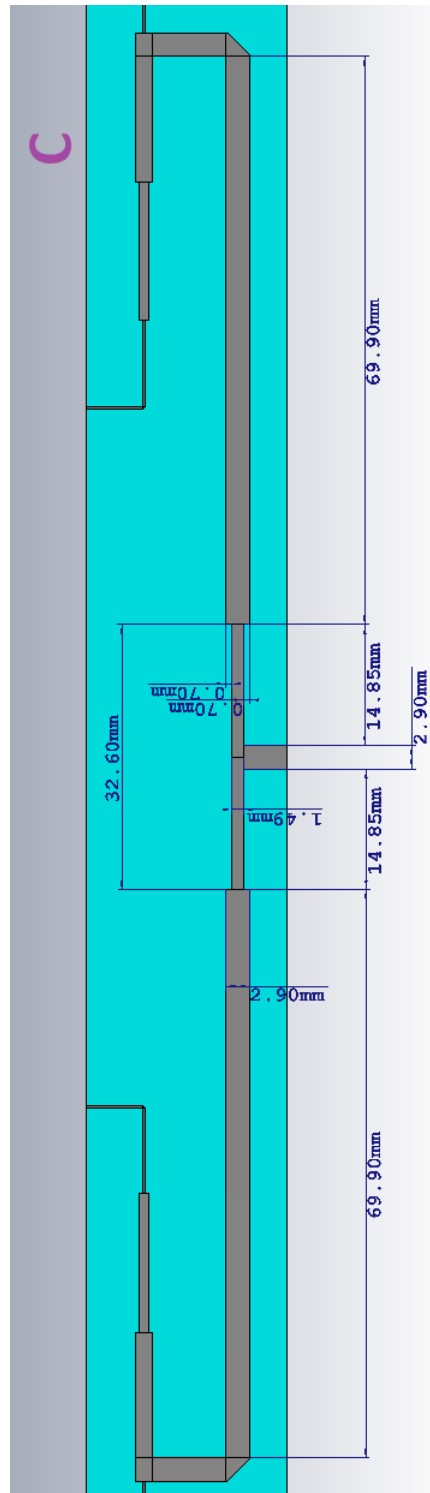


Figure 15: Quoted BFN: region C.

3 Problem no.2

3.1 Simulation with *Design Studio*

In order to verify and optimize the design of the BFN we decided to use *CST Design Studio*, one of the various tools offered by *CST Studio Suite*, which allows the user to design a microstrip network via schematic, to optimize it through the embedded optimization tool and then to create a layout of the whole project that can easily be exported in *CST Microwave Studio* for further simulations.

Figure 16 shows how a schematic looks like in *CST Design Studio*. The isolated block is needed in order to assign to the structure fundamental properties such as thickness of the ground plane and dielectric constant of the substrate, while the other blocks build up the whole structure, allowing the creation of lines with assigned width and length and even bends (for example mitered) and junctions.

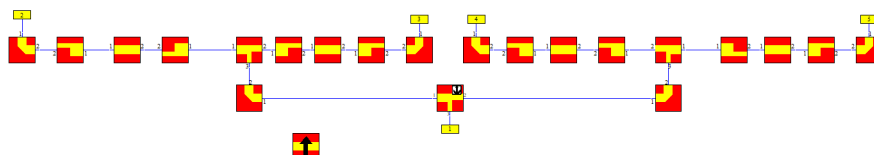


Figure 16: BFN schematic on *CST Design Studio*

As a first step the BFN has been drawn with the dimensions calculated during the design phase and then we specified that we wanted to see the S parameters at all ports (port 1 has an impedance of 50 Ω , ports 2 to 5 have an impedance of 120 Ω , since they take the place of the patches) as a simulation result. Next, the optimizer was set with the initial goal of tuning the S_{11} parameter so to make it resonate at 2.45 GHz with the highest possible precision, obtaining the result shown in figure 17.

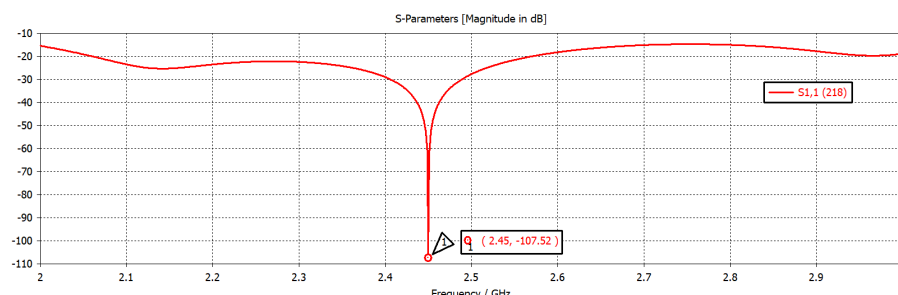


Figure 17: S_{11} parameter of our BFN

As one can see, S_{11} is pretty well shaped and furthermore the resonance at the desired frequency is strong and the obtained bandwidth is quite large.

Next step is the verification of the obtained tapering and phasing, which can be done by checking the value of the S_{ij} parameters.

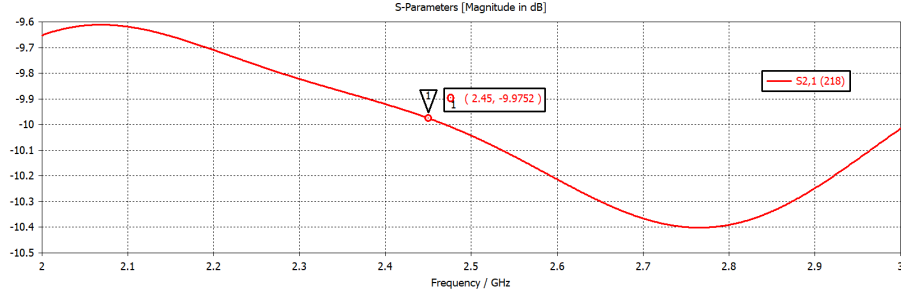


Figure 18: S_{21} parameter of our BFN

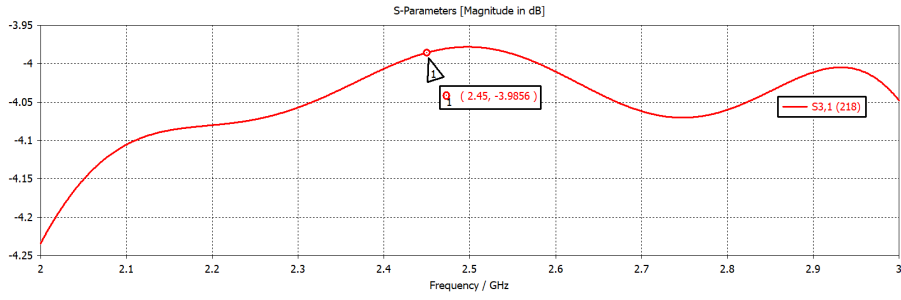


Figure 19: S_{31} parameter of our BFN

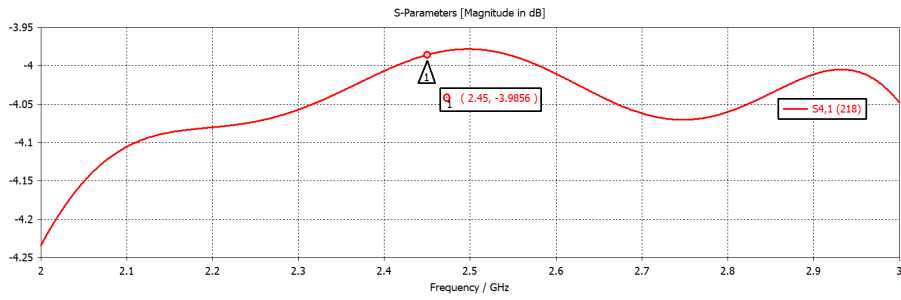


Figure 20: S_{41} parameter of our BFN

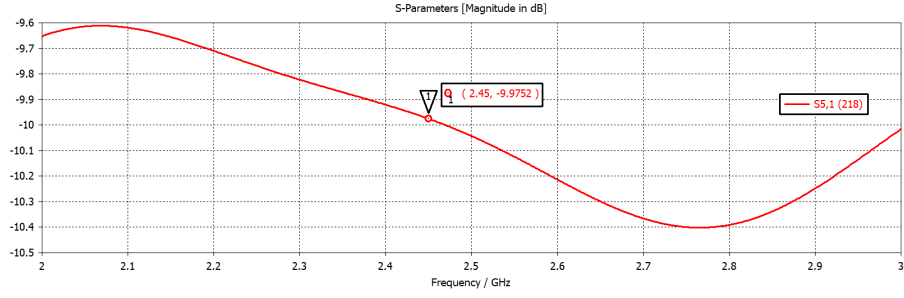


Figure 21: S_{51} parameter of our BFN

The power ratio between the central elements of the array (ports 3 and 4) and the edge ones (ports 1 and 5) turns out to be 5.98 dB.

Last but not least, we have to verify that the phase shift between the output ports is as close as possible to 0.

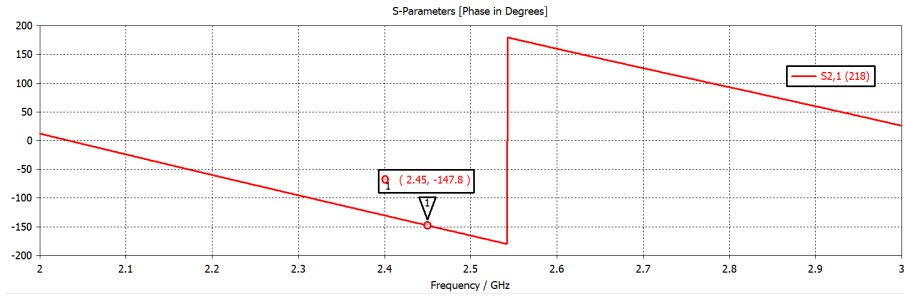


Figure 22: S_{21} parameter (phase), coinciding with S_{51}

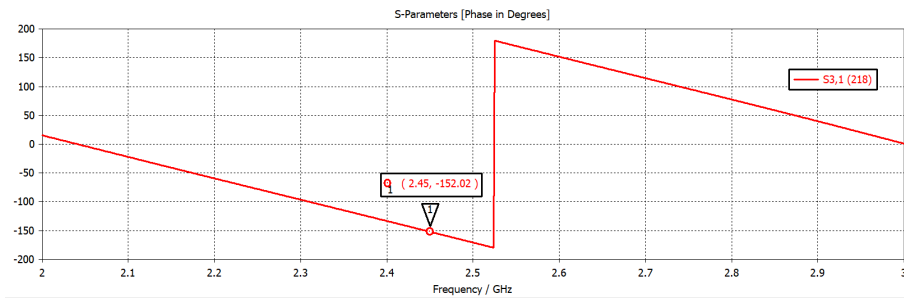


Figure 23: S_{31} parameter (phase), coinciding with S_{41}

The phase difference between center and edge elements is around 4° . A simulation of the complete structure in *Microwave Studio* will tell us whether this lack of precision will affect the behavior of the array a lot or it will result either way to be broadside, as expected.

In order to have a visual impact of what the schematic is translated into in terms of layout, figure 24 shows the resulting structure.

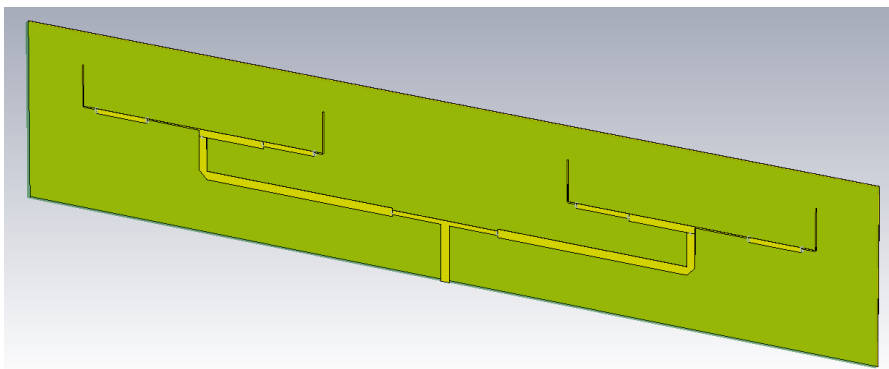


Figure 24: How our BFN looks like

3.2 Simulation with *Microwave Studio*

Unfortunately, if till this point the simulations seemed to be very encouraging, we realized that when trying to transfer the design on *CST Microwave Studio* they were not so good: the resonance was not as precise as we'd have expected and neither was the tapering. Furthermore, if using the optimizer turned out to be a very useful tool when using *Design Studio*, things are not so easy in *Microwave Studio*, where the high density of the mesh needed in order to obtain reliable results makes the simulation time very long. Due to these reasons we began from scratch, trying to build up the single components of the BFN separately. As previously described the power splitters seem to work on their own, giving the correct power ratio and phasing, but even in this case we were not able to put them together obtaining immediately a satisfactory result, nor we managed to optimize the results on the base of what previously obtained as well as we did in *Design Studio*. The reasons are multiple: long simulation time (as already mentioned) if the mesh is dense and low reliability if, with the aim of reducing the simulation time to allow for optimization, one uses a larger meshgrid, very high precision of the optimizer, which specifies a lot of digits (which has no sense if one thinks about the specifications one should give the producer in order to print the antenna). Furthermore: every curve introduces a non ideality and even the simple lines are not easy to tune all together to the correct impedance value. Simulations were carried out both with discrete face ports (whose reference impedance can be specified by the user) and with waveguide ports, with which we were finally able to obtain an acceptable result, even if not perfect as one would like.

In the following figures: the globally best result we obtained in *Microwave Studio*, resonating at the right frequency even if the shape of the curve is

not exceptional and with acceptable tapering:

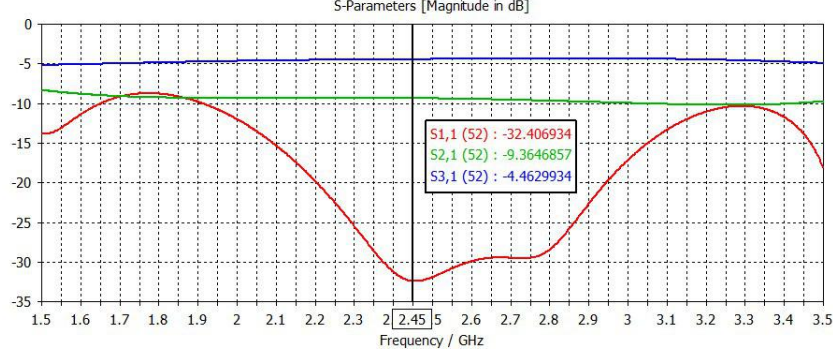


Figure 25: amplitude of the important parameters

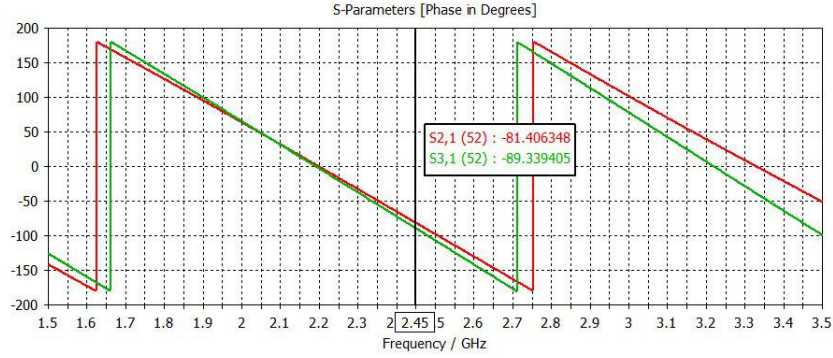


Figure 26: phase of the important parameters

It is important to notice that S_{21} coincides with S_{51} , while S_{31} coincides with S_{41} . This was predictable, but it is also due to the fact that we imposed as a boundary condition a symmetry plane (xy) for the magnetic field, since the symmetry of the system allows for it: the field lines are closed around the microstrip at the input port and the tangent component is null in the xy plane.

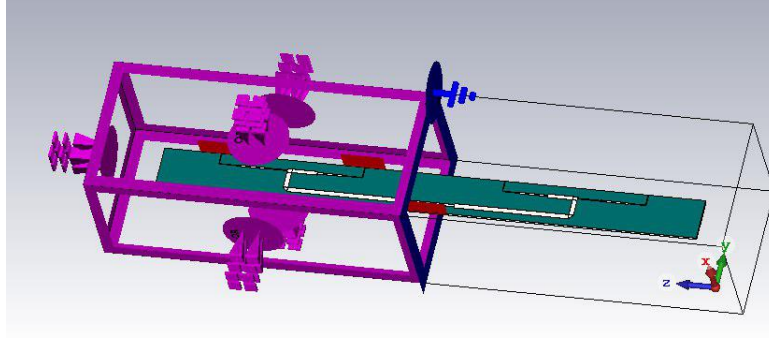


Figure 27: simmetry plane adopted

We also tried to simulate the behavior of the BFN when attached to the patches, but, since the tapering was not the good one we had hoped for, the SLL wasn't completely tuned on the -20 dB level either. Good notes are the fact that the radiated field happened to be broadside, meaning that the phasing, at least, was correct, and that the resonance frequency, even if not perfect, happened to be more precise in this case. A more specific and precise analysis of the obtained AF will be discussed in the last part.

4 Problem no.3

In this last part the aim is to verify the radiating element behavior, starting from the single patch and arriving to the complete array. For the patch antenna we use the one we designed for the second laboratory, that are described in the following image (Figure 28 shows the patch with the values after the first optimization and figure 29 the mesh with the particular of the feeding line).

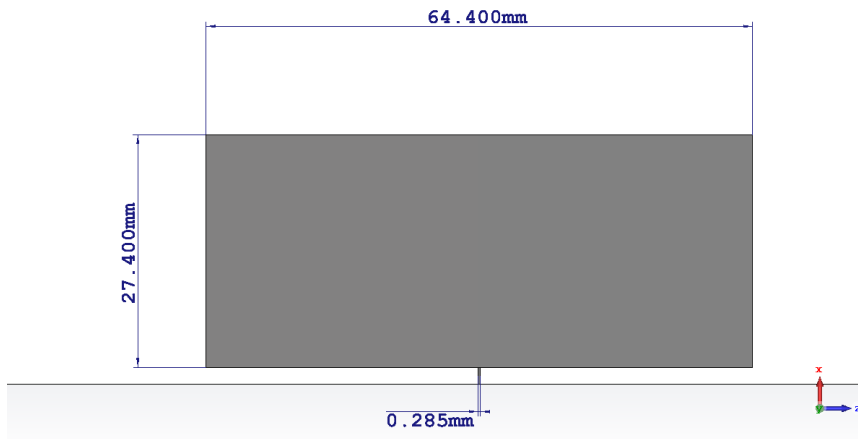


Figure 28: patch resonant at $2.45GHz$

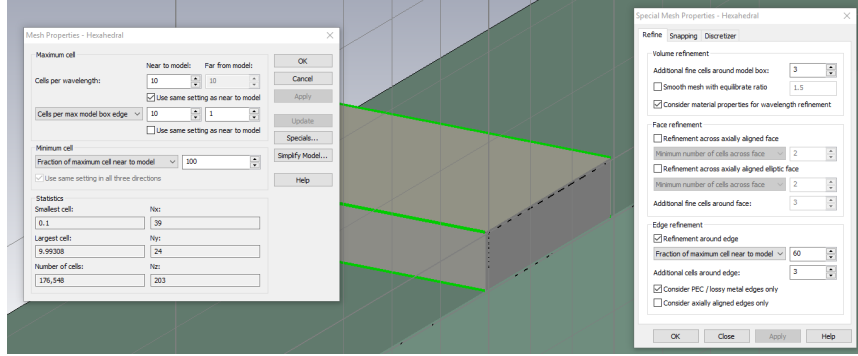


Figure 29: mesh used for the patch

single antenna First of all we analyze the single antenna itself, so that we control it resonates at the correct frequency with our feeding. We use a very short line with characteristic impedance close to the patch output one, in order to simulate the effective feeding that will be implemented with the beam forming network. This choice is made also to minimize the contribution due to the mismatching of the load the line, and in fact the length of the microstrip feeding is much less than λ .

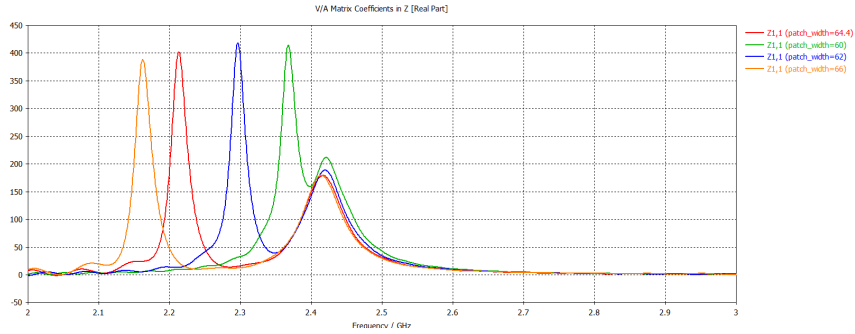


Figure 30: real part of Z_{11} of the single patch. the parameter that is switching is the width of the antenna

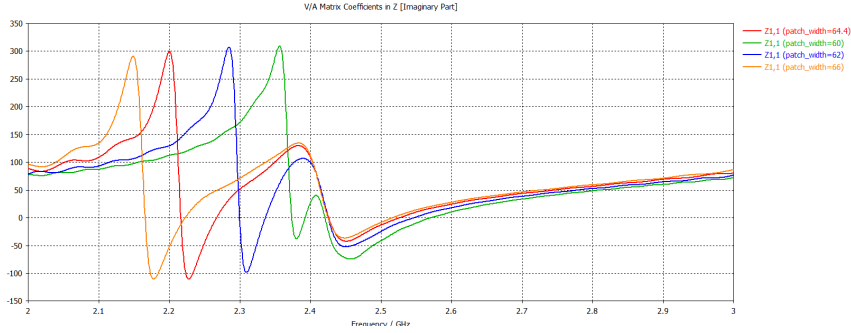


Figure 31: imaginary part of Z_{11} of the single patch. the parameter that is switching is the width of the antenna

We simulate the antenna scattering parameter, and with this simulation we verify the correct resonance at $2.45GHz$ with an input impedance close to 120Ω . On the figure 30 is possible to see some value of this first simulation. Important to notice that the impedance is not exactly 120Ω . This value is hard to reach and tends to block at almost 160Ω when the width is near to $64.4mm$. On the other side as we can see on figure 31 the resonance is a bit before the wanted frequency, but in this case we don't want to optimize the length before simulating the inter elements effects (those contribution could increase the resonance frequency).

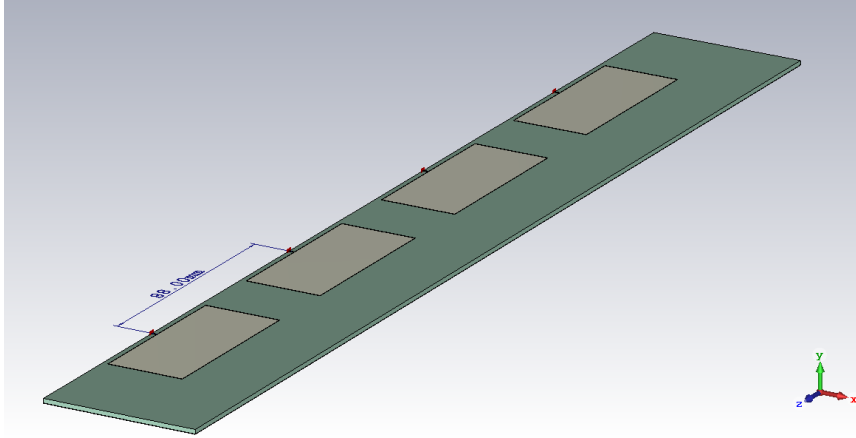


Figure 32: patch resonant at $2.45GHz$

multiple antennas Composing the array with those antennas we can have a first simulation of the complete radiating element, and so we can make some considerations. The bigger issue in particular are the resonance frequency, which due to the inter elements coupling (as expected) are deviated from the single antenna case. In particular the resonance frequency results shifted of few hundreds of megahertz upward, movement that we have to take in

mind in case we want to re-design a similar patch antenna complying better with the specifications.

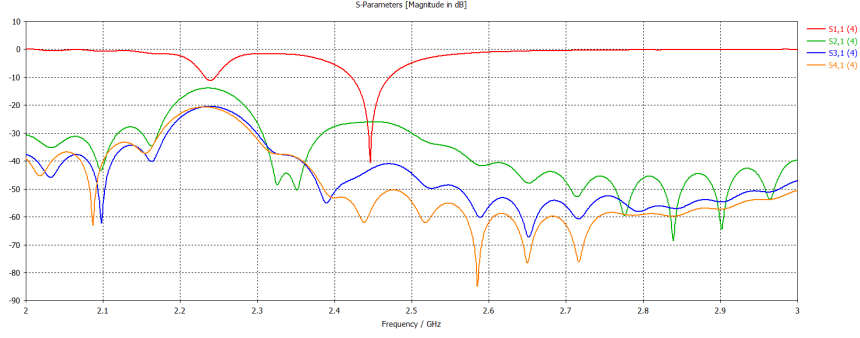


Figure 33: all the scattering parameters with feeding on port 1

Simulating the four antennas with their entering ports we have a total number of 16 scattering parameters, which are not so easy to handle in order to find the load seen from the beam forming network point of view and optimize it. Because we use a constant tapering for the antennas feeding we can combine the results of this simulation and find only four scattering parameters describing the reflection coefficient of each port. This way we can also find the correlated impedance, so that in our particular case of feeding we can evaluate precisely the active impedance of the antennas. The value founded using the tapering evaluated in the previous parts of the design are showed in the figures 35 and 34

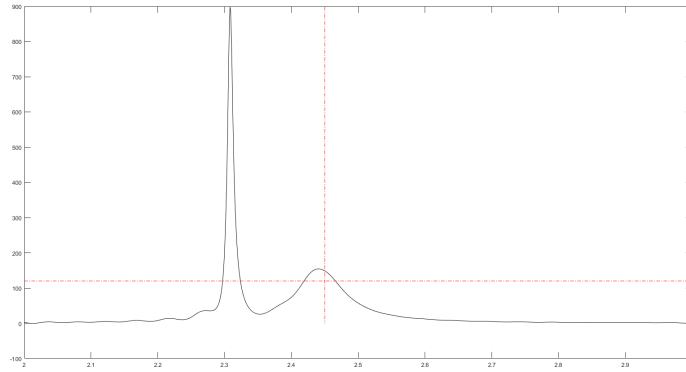


Figure 34: real part of Z_{11} of the array

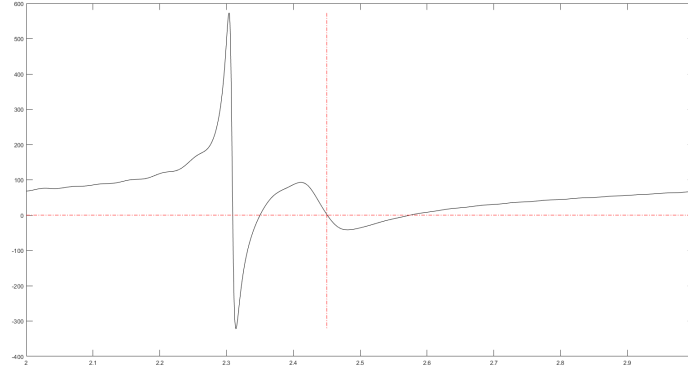


Figure 35: imaginary part of Z11 of the array

Cause of the symmetry of the structure we have that the impedance of the external elements should slightly differs from the internal one, but as we can see on the scattering parameters on the figure 36 the differences are negligible. On top of that we can finally observe, concerning the scattering parameters, that at the wanted frequency we have less than -20dB matching.

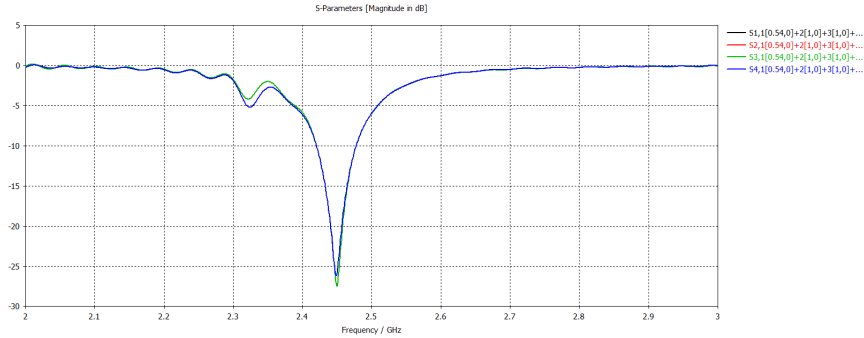


Figure 36: scattering parameters of the array

array factor The last pass is to consider the radiation pattern, which is first of all evaluated with a far field monitor, and after that is exported and elaborated in Matlab in order to verify the correct behavior of the array factor. For this calculation we need also the far field radiation of the single patch antenna, which must be used as a punctual divider for the array far field.

```
1 % import of the data from file exported in ASCII from
  CST
2 data_file='data.txt';
3 data=fopen(data_file, 'r');
```

```

4 fgets(data);
5 fgets(data);
6 data_val=fscanf(data, '%f %f %f %f %f %f %f %f', [8 Inf
]);
7 [~,len]=size(data_val);
8 fclose(data);
9 % prev_val is the set of value taken at the first read
, which in our case
10 % is the radiation pattern of the array
11 figure(1) % rad array
12 plot(prev_val(1,:),prev_val(3,:), 'k', [prev_val(1,1)
prev_val(1,len)], [0 0], '-.r', [2.45 2.45], [min(
prev_val(3,:)) max(prev_val(3,:))], '-.r')
13 figure(2) % rad patch
14 plot(data_val(1,:),data_val(3,:), 'k', [data_val(1,1)
data_val(1,len)], [0 0], '-.r', [2.45 2.45], [min(
data_val(3,:)) max(data_val(3,:))], '-.r')
15 figure(3) %AF
16 plot(data_val(1,:),prev_val(3,:)-data_val(3,:), 'k', [
data_val(1,1) data_val(1,len)], [-20 -20], '-.r', [90
90], [-40 max(data_val(3,:))], '-.r')

```

The result of this calculation is the array factor printed in figure 39, which does not respect the initial requirements for the side lobes (only less than $-15dB$) and the grating lobes (which are evident and arrives at $-5dB$). This optimization, as the one in the previous point, is very long and requires a lot of calculation, so we have to accept this as the best result. Regarding all the other characteristic, the array is verified to work in broadband, and the bandwidth at $-3dB$ is 16° .

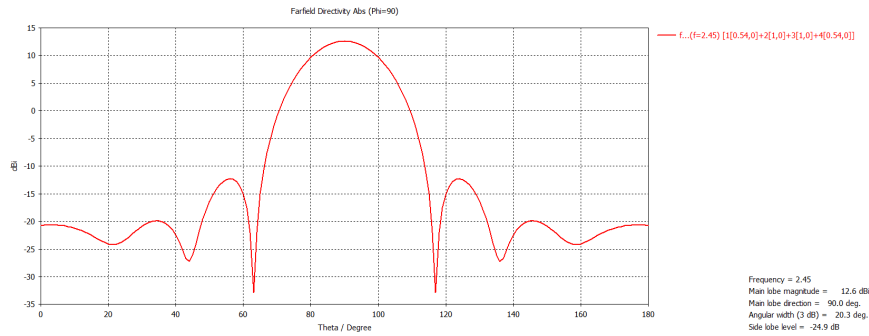


Figure 37: radiation of the array

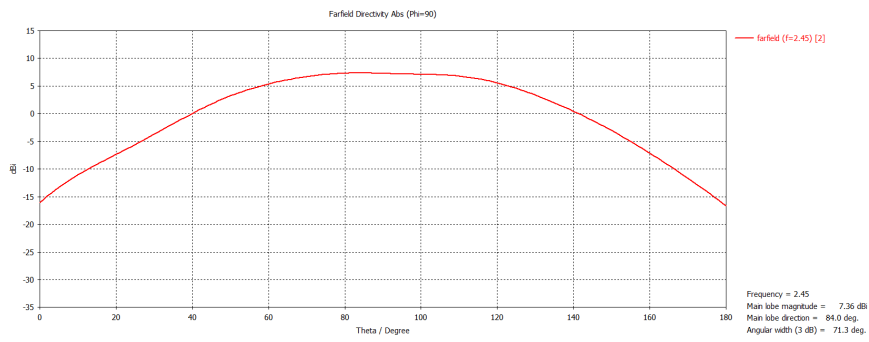


Figure 38: radiation of the single patch

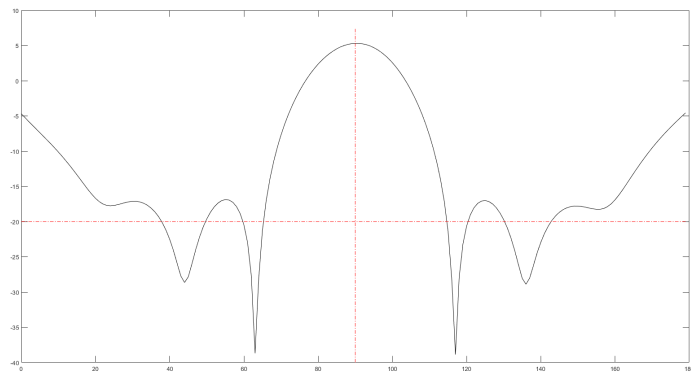


Figure 39: antenna factor of the array